HHS Public Access

Author manuscript

J Dent. Author manuscript; available in PMC 2017 October 01.

Published in final edited form as:

J Dent. 2016 October ; 53: 73–81. doi:10.1016/j.jdent.2016.07.014.

Three-dimensional biofilm properties on dental bonding agent with varying quaternary ammonium charge densities

Han Zhou[1,2], **Huaibing Liu**[3], **Michael D. Weir**[1], **Mary A. Reynolds**[1], **Ke Zhang**[1,4], and **Hockin H. K. Xu**[1,5,6]

[1]Department of Endodontics, Periodontics and Prosthodontics, University of Maryland School of Dentistry, Baltimore, MD 21201, USA

[2]State Key Laboratory of Oral Diseases, West China School of Stomatology, Sichuan University, Chengdu, China

[3]L.D. Caulk Division, Dentsply International, Milford, DE 19963, USA

[4]Department of Orthodontics, School of Stomatology, Capital Medical University, Beijing, China

[5]Center for Stem Cell Biology & Regenerative Medicine, University of Maryland School of Medicine, Baltimore, MD 21201, USA

[6]Department of Mechanical Engineering, University of Maryland, Baltimore County, MD 21250, USA

Abstract

Objectives—Tooth-restoration interfaces are the weak link with secondary caries causing restoration failure. The objectives of this study were to develop an antimicrobial bonding agent with dimethylaminododecyl methacrylate (DMAHDM), and investigate the effects of quaternary amine charge density on three-dimensional (3D) biofilms on dental resin for the first time.

Methods—DMAHDM was synthesized and incorporated into Scotchbond Multi-Purpose bonding agent at mass fractions of 0% (control), 2.5%, 5%, 7.5% and 10%. *Streptococcus mutans* bacteria were inoculated on the polymerized resin and cultured for two days to form biofilms. Confocal laser scanning microscopy was used to measure biofilm thickness, live and dead biofilm volumes, and liv bacteria percentage in 3D biofilm vs. distance from resin surface.

Results—Charge density of the resin had a significant effect on the antibacterial efficacy ($p < 0.05$). Biofilms on control resin had the greatest thicknesses. Biofilm thickness and live biofilm volume decreased with increasing surface charge density ($p < 0.05$). There were significant variations in bacterial viability along the 3D biofilm thickness ($p < 0.05$). At 2.5% and 5% DMAHDM, the bacterial inhibition was the greatest on or near the resin surface, and the killing

Correspondence: Dr. Ke Zhang, Department of Orthodontics, School of Stomatology, Capital Medical University, Beijing, China (tuzizhangke@163.com); Dr. Hockin H. K. Xu, University of Maryland Dental School, Baltimore, MD 21201 (hxu@umaryland.edu).

effect decreased away from the resin surface. At 10% DMAHDM, the entire 3D biofilm was dead and the percentage of live bacteria was nearly 0% throughout the biofilm thickness.

Conclusions—Adding new antibacterial monomer DMAHDM into dental bonding agent yielded a strong antimicrobial activity, substantially decreasing the 3D biofilm thickness, live biofilm volume, and percentage of live bacteria on cross-sections through the biofilm thickness.

Significance—Novel DMAHDM-containing bonding agent with capability of inhibiting 3D biofilms is promising for a wide range of dental restorative and preventive applications to inhibit biofilms at the tooth-restoration margins and prevent secondary caries.

Keywords

Three-dimensional biofilm; quaternary amine charge density; antibacterial bonding agent; biofilm structure; *Streptococcus mutans*; dental caries

1. Introduction

Tooth decay is a prevalent problem worldwide, and the tooth cavities are increasingly being restored using resin composites, due to their good esthetics and direct-filling and photo-polymerization capabilities [1–4]. The composite restorations are bonded to the tooth structures via bonding agents [5–7]. However, recurrent (secondary) caries at the bonded interface has been shown as a main reason for the failure of restorations [3,5,8,9]. Indeed, approximately 50–70% of all tooth cavity restorations were made to replace the failed restorations [10,11]. Dental caries is related to oral biofilms which can produce organic acids and enzymes to cause dissolution of tooth minerals [12]. Therefore, efforts were made to synthesize antibacterial resins to suppress biofilms and acid production [13,14]. A promising approach was to develop quaternary ammonium methacrylates (QAMs) which can be covalently bonded and immobilized in dental resins to provide antimicrobial functions to dental restorations [15–22].

The mode of action for quaternary ammonium was suggested to be that when the negatively-charged bacterial cell contacts the positively-charged sites of the quaternary ammonium, the electric balance of the cell membrane could be disturbed, leading to membrane rupture and cell death [16,23]. Therefore, the quaternary amine charge density of a dental resin would be a key factor in its antimicrobial potency. Indeed, the effects of charge density was shown to be important in several previous studies [18,24–26]. The charge density of poly(4-vinyl-N-alkylpyridinium bromide)-coated glass slide was calculated as an index of surface properties [24]. In another study, the charge density of a resin was shown to increase with greater QAM concentrations in the resin [18]. Furthermore, increasing the quaternary amine charge density of dentin bonding resin greatly reduced the biofilm attachment and growth, without compromising the dentin bond strength [25,26].

However, to date, a literature search revealed no report on the investigation of the effect of charge density on the three-dimensional (3D) biofilm structure and live/dead bacteria viability distribution in biofilms on dental resins. In most previous studies, two-dimensional (2D) images of the external surfaces of the biofilms or the structure of a single bacterial cell were studied using light, scanning and transmission electron microscopy techniques [27,28].

Several studies used confocal laser scanning microscopy (CLSM) to investigate oral biofilms [29–36]. An advantage of CLSM is the horizontal and vertical optical sectioning of the 3D biofilm. The 2D images of thin sections throughout the biofilm can then be used to reconstruct the 3D biofilm structure. In addition, image-processing techniques can be used for quantitative analysis of biofilms to obtain a detailed visualization of thick biofilm samples [37], which cannot be obtained via conventional phase contrast or fluorescence microscopy. While the 3D viability distributions in dental biofilms were studied via CLSM techniques previously [32,33,38,39], to date, there has been no report on the effect of quaternary amine charge density of dental resin on the 3D viability distribution of biofilms.

Accordingly, the objectives of this study were to incorporate QAM into dental bonding agent, and investigate the quaternary amine charge density effect on 3D biofilms on dental resin for the first time. It was hypothesized that: (1) Increasing the quaternary amine charge density would decrease the viability of 3D biofilms on resin; (2) Quaternary amine charge density on resin would significantly influence biofilm thickness as well as live and dead biofilm volumes; (3) In the 3D biofilm, there would be less live bacteria in biofilm bottom near the resin surface, and the percentage of live bacteria would increase with increasing distance away from the resin.

2. Materials and methods

2.1. Synthesis of DMAHDM and antibacterial bonding agent

An antimicrobial monomer, dimethylaminododecyl methacrylate (DMAHDM) with an alkyl chain length of 16, was recently synthesized [40]. DMAHDM was made using a modified Menschutkin reaction, where a tertiary amine was reacted with an organo-halide [18,19]. Briefly, 10 mmol of 1-(dimethylamino)docecane (Sigma, St. Louis, MO) and 10 mmol of 1-bromohexadecane (BHD, TCI America, Portland, OR) were combined with 3 g of ethanol in a 20 mL scintillation vial. The vial was stirred at 70 °C for 24 h. The solvent was then removed via evaporation, yielding DMAHDM as a clear, colorless, and viscous liquid. Details of this method were described recently [18,19,40].

Scotchbond Multi-Purpose (3M, St. Paul, MN) was used as the parent system (referred as “SBMP”) to test the effect of DMAHDM incorporation. According to the manufacturer, SBMP primer contained 35–45% of HEMA, 10–20% of a copolymer of acrylic and itaconic acids, and 40–50% water. SBMP adhesive contained 60–70% of bisphenol A diglycidyl methacrylate (BisGMA), 30–40% of 2-hydroxyethyl methacrylate (HEMA), tertiary amines and photo-initiator. DMAHDM was mixed into primer at DMAHDM/(SBMP primer + DMAHDM) mass fractions of 2.5%, 5%, 7.5%, and 10%. Similarly, DMAHDM was mixed into adhesive at DMAHDM/(SBMP adhesive + DMAHDM) mass fractions of 2.5%, 5%, 7.5%, and 10%. The 10% mass fraction followed previous studies [20,21]. These four mass fractions and the control (0%) allowed the examination of the effect of surface charge density. Five groups were tested:

1. SBMP primer and adhesive (0% DMAHDM, referred to as “SBMP control”);
2. SBMP primer + 2.5% DMAHDM, SBMP adhesive + 2.5% DMAHDM (referred to as “SBMP+2.5DMAHDM”);

3. SBMP primer + 5% DMAHDM, SBMP adhesive + 5% DMAHDM (referred to as “SBMP+5DMAHDM”);
4. SBMP primer + 7.5% DMAHDM, SBMP adhesive + 7.5% DMAHDM (referred to as “SBMP+7.5DMAHDM”);
5. SBMP primer + 10% DMAHDM, SBMP adhesive + 10% DMAHDM (referred to as “SBMP+10DMAHDM”).

2.2. Resin specimen fabrication

Resin disks were made using the cover of a sterile 96-well plate as molds [25,40]. Following previous studies, 10 μL of primer was brushed onto the bottom of a dent of approximately 8 mm in diameter [25,40]. The primer was dried with a stream of air, and then 20 μL of adhesive was applied. A Mylar strip was used to cover the adhesive which was then light-cured for 20 s (Optilux VCL 401, Demetron Kerr, Danbury, CT). This yielded a cured resin disk of approximately 8 mm in diameter and 0.5 mm in thickness [40]. The disks were removed from the cover of the 96-well plate, immersed in 200 mL of distilled water, and stirred via a magnetic stirrer at a speed of 100 rpm (Bellco Glass, Vineland, NJ) for 1 h to remove any uncured monomers, following a previous study [15]. The purpose of this was to avoid complications from the release of uncured monomers which could have moderate antibacterial effects, so that the measured antibacterial properties were due to the polymerized QAM in the resin and not due to uncured monomer release during biofilm cultures. The disks were dried, sterilized in an ethylene oxide sterilizer (Anprolene AN 74i, Andersen, Haw River, NC), de-gassed for 7 d and then used in biofilm experiments.

2.3. Quaternary amine charge density of bonding agent containing DMAHDM

The density of quaternary ammonium groups present on the polymer surfaces was quantified using a fluorescein dye method [18,24,25]. Resin disks of each bonding agent group were placed in a 48-well plate. Fluorescein sodium salt (200 μL of 10 mg/mL in deionized water) was added into each well, and specimens were left for 10 min at room temperature in the dark. After removing the fluorescein solution and rinsing extensively with water, each sample was placed in a new well, and 200 μL of 0.1% (by mass) of cetyltrimethylammonium chloride (CTMAC) in DI water was added. Samples were shaken for 20 min at room temperature in the dark to desorb the bound dye. The CTMAC solution was supplemented with 10% (by volume) of 100 mM phosphate buffer at pH 8. This was prepared with 0.94 mg/mL monosodium phosphate-monohydrate and 13.2 mg/mL disodium phosphate-anhydrous in DI water. Sample absorbance was read at 501 nm using a plate reader (SpectraMax M5, Molecular Devices, Sunnyvale, CA) [24,25]. The fluorescein concentration was calculated using Beers Law and an extinction coefficient of 77 mM^{-1} cm^{-1} [18,25]. Using a ratio of 1:1 for fluorescein molecules to the accessible quaternary ammonium groups, charge density was calculated as the total molecules of charge per exposed surface area. The surface area was equal to the summation of top, bottom and side areas, measured for each disk due to slight variations in disk sizes [25].

2.4. Confocal laser scanning microscopy (CLSM) analysis of 3D biofilms

The use of *Streptococcus mutans* (*S. mutans*) bacteria (ATCC700610, American Type, Manassas, VA) was approved by the University of Maryland Baltimore Institutional Review Board. A 15 μL of *S. mutans* stock bacteria was added to 15 mL of brain heart infusion broth (BHI, Becton, Sparks, MD) and incubated at 37 °C with 5% CO_2 for 16 h. 150 μL of this *S. mutans* suspension was then diluted by 10-fold in a growth medium which consisted of BHI supplemented with 0.2% sucrose to form *S. mutans* inoculation medium of 1.5 mL [25].

Each resin disk was placed in a well of a 24-well plate and inoculated with 1.5 mL of the *S. mutans* inoculation medium. The samples were incubated at 5% CO_2 and 37 °C. The medium consisted of BHI with 0.2% sucrose. After 8 h, the disks were transferred to new 24-well plates with fresh medium [19,21–25]. After 16 h, the disks were transferred to new 24-well plates and incubated for 24 h. This totaled two days of culture which was shown previously to form biofilms on dental resins [19,21–25]. The biofilms on resin disks were washed with phosphate buffered saline (PBS) to remove the loose bacteria. Disks with adherent biofilms were stained using a BacLight live/dead kit (Molecular Probes, Eugene, OR). Live bacteria were stained with Syto 9 to produce a green fluorescence. Bacteria with compromised membranes were stained with propidium iodide to produce a red fluorescence [19,21–25].

The biofilms were investigated using a 3D model as previously described [41,42]. The fluorescence was examined using a confocal laser scanning microscope (CLSM, LSM510, Carl Zeiss, Thornwood, NY). Green fluorescence was provided with an argon laser (488-nm laser excitation), and red fluorescence was given with a helium-neon laser (543 nm laser excitation). Images were taken from the bottom of the biofilm that was in contact with the resin disk surface, and then section by section toward the top surface of the biofilm. The biofilm section parallel to the resin surface was referred to as the x–y plane, and the direction perpendicular to the resin surface was called the z axis [42]. For each biofilm, 10 planes at equal distances along the z axis were imaged [42]. These 2D sections were stacked and reconstructed to form a 3D image of the biofilm using the IMARIS software (Bitplane, Saint Paul, MN) [42]. The biofilm images were analyzed using a software (bioImageL, Faculty of Odontology, Malmö University, Malmö, Sweden) [37]. The bioImageL software is based on color segmentation algorithms written in MATLAB (MathWorks, Natick, MA) and can produce information of the structure and spatial differences in biofilm. The biofilm is characterized by parameters including biofilm thickness, green-stained live bacteria volume, red-stained dead bacteria volume, as well as the live and dead bacteria coverage on each two-dimensional x–y section along the biofilm thickness [42].

2.5. Statistical analysis

Statistical analyses were performed using SPSS 17.0 software (SPSS, Chicago, IL). Two-way analysis of variance (ANOVA) was used to examine the data in Fig. 6 on the effects of resin surface charge density and location in 3D biofilm. One way ANOVA was used to analyze all other data. Tukey's multiple comparison tests were performed to detect significant effects of the variables using a p value of 0.05.

3. Results

The quaternary amine surface charge density of the cured bonding agent resin disks is plotted in Fig. 1(A) (mean ± sd; n = 6). Fluorescein binding to the cationic quaternary groups showed more quaternary ammonium sites on resin with increasing DMAHDM mass fraction ($p < 0.05$). The control group with 0% DMAHDM had some nonspecific interactions with the fluorescein salt resulting in a small charge density value of slightly greater than 0. However, what should be noted is that even when compared with the group containing 2.5% DMAHDM, the specimens containing 10% DMAHDM had about 5 times more quaternary ammonium sites present on the resin surface. These results showed that increasing the DMAHDM mass fraction in the resin successfully increased the quaternary amine surface charge density.

The 3D biofilm thickness results are plotted in Fig. 1(B) (mean ± sd; n = 6). Increasing the DMAHDM mass fraction decreased the biofilm thickness ($p < 0.05$), from being thicker than 40 μm for SBMP control without DMAHDM, to about 10 μm thickness for the resin containing 10% DMAHDM.

Representative 3D images of biofilms on resins are shown in Fig. 2: (A) SBMP control, (B) SBMP+2.5DMAHDM, (C) SBMP+5DMAHDM, (D) SBMP+7.5DMAHDM, and (E) SBMP+10DMAHDM. The x–y plane is parallel to the resin surface, the z axis is perpendicular to resin surface, and z = 0 is on the resin surface. SBMP control had primarily live bacteria. The amount of live bacteria progressively decreased, and the dead bacteria gradually increased, with increasing DMAHDM mass fraction. At 7.5% and 10% DMAHDM, there were primarily dead bacteria. The z axis measurement indicated that the 3D biofilms on SBMP control were the thickest, and the biofilm thickness steadily decreased with increasing DMAHDM content.

Fig. 3 plots the biofilm volume results: (A) Live biofilm volume, and (B) dead biofilm volume (mean ± sd; n = 6). In (A), the live biofilm volume progressively decreased with increasing the DMAHDM mass fraction, by two orders of magnitude from SBMP control to SBMP+10DMAHDM. In (B), the dead biofilm volume increased by more than an order of magnitude from SBMP control to the other groups containing DMAHDM ($p < 0.05$). The groups containing various amounts of DMAHDM had relatively small variations in the dead biofilm volume values, but were within the same order of magnitude.

Fig. 4 shows typical live/dead images of 2D x–y sections of the top biofilm surface, the middle biofilm section, and the bottom biofilm section (on resin surface) for: (A) SBMP control, (B) SBMP+5DMAHDM, and (C) SBMP+10DMAHDM. In (A), the top surface of biofilm on SBMP had the most live bacteria, the middle section of biofilm was also primarily alive, while the biofilm bottom on resin had compromised bacteria with isolated red/orange staining. In (B), the top surface of the biofilm had more green staining areas than red, but the bottom of the biofilm had more dead bacteria than live bacteria. In (C), the biofilm top, middle section and bottom all contained compromised bacteria. There were little, if any, live bacteria throughout the biofilm. SBMP+2.5DMAHDM (not shown) had biofilm features that was intermediate and between those of SBMP control and SBMP

+5DMAHDM. SBMP+7.5DMAHDM (not shown) had biofilm features in between those on SBMP+5DMAHDM and SBMP+10DMAHDM.

Fig. 5 plots the biofilm viability distribution through biofilm thickness as a function of z axis height (mean ± sd; n = 6): (A) SBMP control, (B) SBMP+2.5DMAHDM, (C) SBMP +5DMAHDM, (D) SBMP+7.5DMAHDM, and (E) SBMP+10DMAHDM. The vertical axis shows the percentage of live bacteria measured from 2D sections such as those in Fig. 4. The horizontal axis indicates the biofilm thickness at which the 2D image was taken. SBMP control had slightly more than 60% of live bacteria at the biofilm bottom; it increased to nearly 100% of live bacteria near the biofilm top. The percentage of live bacteria decreased with increasing DMAHDM mass fraction. At 7.5% DMAHDM, not only did the percentage of live bacteria decrease to 15% at the biofilm bottom, but the top only had 24% live bacteria. At 10% DMAHDM, the percentage of live bacteria was nearly 0% throughout the biofilm thickness.

The percentage of live bacteria in 3D biofilms vs. resin surface charge density is plotted in Fig. 6 (mean ± sd; n = 6). For both the top surface of the 3D biofilm and the bottom section, the percentage of live bacteria decreased with increasing charge density ($p < 0.05$). At each charge density value, the top surface of the 3D biofilm had a greater percentage of live bacteria than the bottom section ($p < 0.05$). The only exception was at the highest charge density tested, when the top of the 3D biofilm and the bottom both had percentages of live bacteria close to 0.

4. Discussion

Dental caries is one of the most common diseases in humans which is caused by oral biofilm acids. Therefore, a promising approach to combat caries is to develop bioactive dental restorations that can suppress biofilms and reduce acid production. This study evaluated the 3D structure of biofilms, live/dead volume and bacterial viability variations through the biofilm thickness on dental resin vs. resin surface charge density for the first time. The results proven the hypotheses that increasing quaternary amine charge density greatly reduced the viability of 3D biofilms on resin; the resin surface charge density affected the biofilm thickness as well as the live and dead biofilm volumes; and there were significantly less live bacteria in the biofilm bottom near the resin surface, than in the portions of the biofilm with increasing distance away from the resin. Increasing the charge density greatly decreased the 3D biofilm thickness, live biofilm volume, and percentage of live bacteria.

Three key points should be discussed here. First, the charge density of the resin had a profound effect on the antibacterial efficacy. In the oral environment, bacteria colonize on teeth and restoration surfaces to form biofilms (plaque). Cariogenic bacteria such as *S. mutans* in the biofilm metabolize carbohydrates and produce acids, leading to tooth decay and secondary caries at the tooth-restoration margins. Therefore, the antibacterial bonding agent containing DMAHDM with an effective biofilm-inhibition capability is promising for suppressing secondary caries at the tooth-restoration margins. The positively-charged quaternary amine N^+ of the antibacterial resin could attract the negatively-charged cell membrane of bacteria, leading to cell membrane rupture and cytoplasmic leakage [16,23]. In

addition, the positively-charged ammonium group interacting with the negatively-charged bacterial membrane could change the balance of the essential ions including K^+, Na^+, $Ca^{2+}$and Mg^{2+}, which could interrupt protein activity and damage the bacterial DNA [43]. For example, an antimicrobial polymeric brush with a high density cationic surface was shown to effectively kill bacteria [44]. Therefore, the charge density is an important parameter for antibacterial resins. One study showed that the surface charge density of a resin was increased with increasing the quaternary ammonium dimethacrylate mass fraction [18]. Indeed, the increased surface charge density was shown to enhance the antibacterial potency [25]. However, these studies focused on 2D biofilm surfaces, without investigating the 3D biofilm structure and bacterial viability variation as a function of resin surface charge density.

The present study demonstrated that the 3D structural changes in biofilms were associated with the surface charge density of dental bonding agent. With DMAHDM mass fraction in resin increasing from 0% to 10%, the charge density increased to 7×10^{15} N^+/cm^2. This resulted in a precipitous decrease in biofilm thickness, live biofilm volume, and the percentage of live bacteria in cross-sections in biofilm thickness. A higher charge density was directly related to a reduced biofilm thickness (Fig. 1). In addition, increasing the surface charge density caused a monotonic decrease in biofilm viability throughout the 3D biofilm thickness (Fig. 6). These results can be explained by the higher DMAHDM concentration yielding more positive charges on the resin to interact with bacteria, leading to a greater antibacterial effect.

Second, there were significant bacterial viability variations along the 3D biofilm thickness. CLSM examination showed that for SBMP control, the bottom layer of the biofilm adjacent to the resin contained a higher proportion of nonviable bacteria than the upper layer of the biofilm in contact with culture medium. This was probably because, compared to the outer layer of the biofilm, the deeper portion of the biofilm had less access to oxygen and nutrients, and more accumulation of secondary metabolites. When biofilms were grown on resins containing DMAHDM, there were more compromised bacteria in the lower part of the biofilm than the outer layer of the biofilm. The percentage of live bacteria increased with the biofilm height in the z axis away from the resin surface. This was likely because of the mechanism of contact-inhibition [13–15], in which the QAM was co-polymerized with, and immobilized in, the resin. The contact-inhibition would imply that the antimicrobial potency would be reduced due to a lack of contact when the bacteria are located in the 3D biofilm away from the resin surface.

Third, for the SBMP+10DMAHDM resin, the entire biofilm was killed and the biofilm consisted of dead microorganisms throughout the biofilm thickness, which may suggest another possible antibacterial mechanism in addition to contact-inhibition. Indeed it was suggested that a stress condition or challenge in bacteria could trigger a built-in suicide program in the biofilm [45,46], which was called the programmed cell death (PCD) [44]. It was postulated that when a biofilm was challenged by bactericidal agents, this challenge may serve as a trigger for PCD in the surrounding bacteria [45,46]. The fact that the SBMP +10DMAHDM resin killed the entire biofilm, and not just the bacteria in contact with the resin surface, is consistent with a previous study [47]. In that previous intra-oral study using

human participants, oral biofilms on an antimicrobial composite containing QAM was killed not only on the resin surface, but also in the outer, more remote parts of the biofilm [47]. This outcome was explained as because of an intracellularly-mediated death program, in which the bacterial lysis by QAM on the resin surface may function as a stressful condition triggering PCD to the bacteria further away in the biofilm [47]. While the previous study [47] is consistent with the present study on 3D biofilm analysis on SBMP+10DMAHDM, the previous study did not investigate the effect of charge density on 3D biofilms. The present study indicated that this possible mechanism of intracellularly-mediated death program to trigger PCD to the bacteria further away in the biofilm may be dependent on the surface charge density (or the severity of the challenge). It appeared that only when a threshold charge density was exceeded would this PCD be triggered. This is because only SBMP+10DMAHDM resulted in the death of the entire 3D biofilm; SBMP+7.5DMAHDM had a biofilm that was almost entirely dead; while SBMP+2.5DMAHDM and SBMP +5DMAHDM had biofilms that were mostly alive in areas away from the resin surface. However, further study is needed to determine if there is a threshold surface charge density to trigger an intracellularly-mediated death in 3D oral biofilms. In addition, further investigation is also needed to verify the killing of bacteria throughout the 3D biofilm thickness in the oral environment *in vivo*.

The present study incorporated 10% by mass of DMAHDM into a bonding agent, following a previous study [40]. While the present study focused on charge density effects on 3D biofilms without investigating whether DMAHDM was adequately polymerized into the resin matrix, two factors appear to support the DMAHDM polymerization in the resin. First, a previous study used 10% DMAHDM in bonding agent and measured the dentin bond strength using extracted human teeth [40]. The dentin was bonded, photo-polymerized, and tested. The microtensile dentin bond strength of bonding agent containing 10% DMAHDM was the same as that of the control bonding agent with 0% DMAHDM. This indicates that the 10% DMAHDM in bonding agent was adequately polymerized. If significant amounts of the 10% DMAHDM in bonding agent had not been polymerized, the dentin bond strength would have been adversely affected. Second, the photo-polymerized bonding agent resin disks containing 10% DMAHDM were immersed in 50 mL culture media and agitated for 24 hours at 37 °C to obtain eluents, which were then used to culture human fibroblasts and odontoblasts [40]. There was no difference in cell viability for the resin with 10% DMAHDM, compared to that with 0% DMAHDM. Hence the eluent from the resin with 10% DMAHDM was similar to that with 0% DMAHDM, indicating that the bonding agent containing 10% DMAHDM was adequately polymerized. If significant amounts of the 10% DMAHDM in the bonding agent had not been polymerized, there would have been much more uncured DMAHDM in the eluent, which would have significantly decreased the cell viability. Further study is needed to directly determine the DMAHDM polymerization in the resin matrix and its degree of conversion.

Dental bonding agents containing DMAHDM with strong antimicrobial functions are promising for a range of applications, including bonding a restoration to tooth structures, and as a crown cement, orthodontic cement, pit and fissure sealant, and tooth root surface coatings. For example, after the tooth cavity is prepared, the antibacterial bonding agent in the unpolymerized state could flow into dentinal tubules to kill residual bacteria in the tooth

cavity [14,15,48,49]. Furthermore, after placement of the bonding agent and composite with photo-polymerization, the antibacterial bonding agent in the polymerized state could combat bacteria invasion along the margins, as marginal microgaps often occur during service over time [14,15,48,49]. In addition, in clinics, there is an increased interest in the less removal of tooth structures and minimal intervention dentistry to preserve tooth structures [50]. However, this could cause more carious tissues to remain along with bacteria in the cavity. In particular, atraumatic restorative treatment (ART) does not require electricity and running water and hence can be performed in developing countries and remote villages, but ART does not completely remove the carious tissues, with remnants of lesions and bacteria in the tooth cavity [51]. Therefore, a bonding agent containing DMAHDM, which was shown to effectively inhibit 3D biofilms in the present study, may be useful for ART and other treatments, especially for certain populations in poverty where caries occurrence is high and oral biofilms and plaque buildups are more prevalent. Further investigation is needed to examine dental applications of DMAHDM-containing resins including long-term durability and *in vivo* tests.

5. Conclusions

This study investigated surface charge density effects of dental resins on 3D biofilm structure and live/dead viability variations through the biofilm thickness for the first time. DMAHDM was incorporated into bonding agent at different mass fractions thus enabling a series of quaternary amine charge densities on the resin to be tested. Increasing surface charge density on bonding agent greatly reduced biofilm growth and viability. Biofilm thickness and live biofilm volume decreased with increasing charge density. For the majority of the tested antibacterial bonding agents, the bacteria inhibition efficacy was the greatest on or near the resin surface, and the killing effect decreased in the 3D biofilm away from the resin surface. However, for the bonding agent containing 10% DMAHDM, the entire 3D biofilm was dead and the percentage of live bacteria was nearly 0% throughout the 3D biofilm. These results indicate that 3D biofilm analysis is useful for understanding dental resin-biofilm interactions, and 2D observations on the top surface of biofilms are insufficient. Novel DMAHDM-containing antimicrobial bonding agent is promising for a range of dental applications to inhibit biofilms at tooth-restoration margins and prevent secondary caries. DMAHDM may be useful in a variety of bonding agents, cements, sealants and composites to inhibit caries.

Acknowledgments

We thank Drs. Lei Cheng and Fang Li for discussions. We are grateful to Dr. Dean Dessem for help with the confocal laser scanning microscope. This study was supported by NIH R01 DE17974 (HX), West China School of Stomatology (HZ), National Natural Science Foundation of China grant 81400540 (KZ), Beijing Municipal Administration of Hospitals' Youth Program QML20151401 (KZ), and a seed grant from the University of Maryland Baltimore School of Dentistry (HX).

References

1. Drummond JL. Degradation, fatigue, and failure of resin dental composite materials. J Dent Res. 2008; 87:710–9. [PubMed: 18650540]

2. Lynch CD, Frazier KB, McConnell RJ, Blum IR, Wilson NH. State-of-the-art techniques in operative dentistry: contemporary teaching of posterior composites in UK and Irish dental schools. Br Dent J. 2010; 209:129–36. [PubMed: 20706252]

3. Ferracane JL. Resin composite--state of the art. Dent Mater. 2011; 27:29–38. [PubMed: 21093034]

4. Demarco FF, Correa MB, Cenci MS, Moraes RR, Opdam NJ. Longevity of posterior composite restorations: not only a matter of materials. Dent Mater. 2012; 28:87–101. [PubMed: 22192253]

5. Spencer P, Ye Q, Park J, Topp EM, Misra A, Marangos O, Wang Y, Bohaty BS, Singh V, Sene F, Eslick J, Camarda K, Katz JL. Adhesive/Dentin interface: the weak link in the composite restoration. Ann Biomed Eng. 2010; 38:1989–2003. [PubMed: 20195761]

6. Pashley DH, Tay FR, Breschi L, Tjaderhane L, Carvalho RM, Carrilho M, Tezvergil-Mutluay A. State of the art etch-and-rinse adhesives. Dent Mater. 2011; 27:1–16. [PubMed: 21112620]

7. Sadeghi M, Davari A, Lynch CD. The effect of re-bonding using surface sealant or adhesive system on microleakage of class V resin composite restorations. Dent Res J. 2013; 10:596–601.

8. Mjor IA, Toffenetti F. Secondary caries: a literature review with case reports. Quintessence Int. 2000; 31:165–79. [PubMed: 11203922]

9. Sakaguchi, RL. Dent Mater; Review of the current status and challenges for dental posterior restorative composites: clinical, chemistry, and physical behavior considerations. Summary of discussion from the Portland Composites Symposium (POCOS); June 17–19, 2004; Portland, Oregon: Oregon Health and Science University; 2005. p. 3-6.

10. Frost PM. An audit on the placement and replacement of restorations in a general dental practice. Prim Dent Care. 2002; 9:31–6. [PubMed: 11901789]

11. Bagramian RA, Garcia-Godoy F, Volpe AR. The global increase in dental caries. A pending public health crisis. Am J Dent. 2009; 22:3–8. [PubMed: 19281105]

12. ten Cate JM. Biofilms, a new approach to the microbiology of dental plaque. Odontology. 2006; 94:1–9. [PubMed: 16998612]

13. Antonucci JM, Zeiger DN, Tang K, Lin-Gibson S, Fowler BO, Lin NJ. Synthesis and characterization of dimethacrylates containing quaternary ammonium functionalities for dental applications. Dent Mater. 2012; 28:219–28. [PubMed: 22035983]

14. Imazato S. Antibacterial properties of resin composites and dentin bonding systems. Dent Mater. 2003; 19:449–57. [PubMed: 12837391]

15. Imazato S. Bio-active restorative materials with antibacterial effects: new dimension of innovation in restorative dentistry. Dent Mater J. 2009; 28:11–9. [PubMed: 19280964]

16. Imazato S, Ehara A, Torii M, Ebisu S. Antibacterial activity of dentine primer containing MDPB after curing. J Dent. 1998; 26:267–71. [PubMed: 9594480]

17. Namba N, Yoshida Y, Nagaoka N, Takashima S, Matsuura-Yoshimoto K, Maeda H, Van Meerbeek B, Suzuki K, Takashiba S. Antibacterial effect of bactericide immobilized in resin matrix. Dent Mater. 2009; 25:424–30. [PubMed: 19019421]

18. Xu X, Wang Y, Liao S, Wen ZT, Fan Y. Synthesis and characterization of antibacterial dental monomers and composites. J Biomed Mater Res B Appl Biomater. 2012; 100:1151–62. [PubMed: 22447582]

19. Cheng L, Weir MD, Xu HH, Antonucci JM, Kraigsley AM, Lin NJ, Lin-Gibson S, Zhou X. Antibacterial amorphous calcium phosphate nanocomposites with a quaternary ammonium dimethacrylate and silver nanoparticles. Dent Mater. 2012; 28:561–72. [PubMed: 22305716]

20. Cheng L, Zhang K, Melo MA, Weir MD, Zhou X, Xu HH. Anti-biofilm dentin primer with quaternary ammonium and silver nanoparticles. J Dent Res. 2012; 91:598–604. [PubMed: 22492276]

21. Zhang K, Melo MA, Cheng L, Weir MD, Bai Y, Xu HH. Effect of quaternary ammonium and silver nanoparticle-containing adhesives on dentin bond strength and dental plaque microcosm biofilms. Dent Mater. 2012; 28:842–52. [PubMed: 22592165]

22. Tezvergil-Mutluay A, Agee KA, Uchiyama T, Imazato S, Mutluay MM, Cadenaro M, Breschi L, Nishitani Y, Tay FR, Pashley DH. The inhibitory effects of quaternary ammonium methacrylates on soluble and matrix-bound MMPs. J Dent Res. 2011; 90:535–40. [PubMed: 21212315]

23. Beyth N, Yudovin-Farber I, Bahir R, Domb AJ, Weiss EI. Antibacterial activity of dental composites containing quaternary ammonium polyethylenimine nanoparticles against Streptococcus mutans. Biomaterials. 2006; 27:3995–4002. [PubMed: 16564083]
24. Tiller JC, Liao CJ, Lewis K, Klibanov AM. Designing surfaces that kill bacteria on contact. Proc Natl Acad Sci U S A. 2001; 98:5981–5. [PubMed: 11353851]
25. Li F, Weir MD, Chen J, Xu HH. Effect of charge density of bonding agent containing a new quaternary ammonium methacrylate on antibacterial and bonding properties. Dent Mater. 2014; 30:433–41. [PubMed: 24534376]
26. Zhou H, Li F, Weir MD, Xu HH. Dental plaque microcosm response to bonding agents containing quaternary ammonium methacrylates with different chain lengths and charge densities. J Dent. 2013; 41:1122–31. [PubMed: 23948394]
27. Brecx M, Winkler M, Netuschil L. Human dental plaque formation on plastic films. A quantitative SEM study. J West Soc Periodontol Periodontal Abstr. 1994; 42:77–80. [PubMed: 8531250]
28. Hannig M. Transmission electron microscopy of early plaque formation on dental materials in vivo. Eur J Oral Sci. 1999; 107:55–64. [PubMed: 10102751]
29. Robinson C, Kirkham J, Percival R, Shore RC, Bonass WA, Brookes SJ, Kusa L, Nakagaki H, Kato K, Nattress B. A method for the quantitative site-specific study of the biochemistry within dental plaque biofilms formed in vivo. Caries Res. 1997; 31:194–200. [PubMed: 9165190]
30. Singleton S, Treloar R, Warren P, Watson GK, Hodgson R, Allison C. Methods for microscopic characterization of oral biofilms: analysis of colonization, microstructure, and molecular transport phenomena. Adv Dent Res. 1997; 11:133–49. [PubMed: 9524450]
31. Wood SR, Kirkham J, Marsh PD, Shore RC, Nattress B, Robinson C. Architecture of intact natural human plaque biofilms studied by confocal laser scanning microscopy. J Dent Res. 2000; 79:21–7. [PubMed: 10690656]
32. Gong SQ, Epasinghe J, Rueggeberg FA, Niu LN, Mettenberg D, Yiu CK, Blizzard JD, Wu CD, Mao J, Drisko CL, Pashley DH, Tay FR. An ORMOSIL-containing orthodontic acrylic resin with concomitant improvements in antimicrobial and fracture toughness properties. PLoS One. 2012; 7:e42355. [PubMed: 22870322]
33. Gong SQ, Epasinghe DJ, Zhou B, Niu LN, Kimmerling KA, Rueggeberg FA, Yiu CK, Mao J, Pashley DH, Tay FR. Effect of water-aging on the antimicrobial activities of an ORMOSIL-containing orthodontic acrylic resin. Acta Biomater. 2013; 9:6964–73. [PubMed: 23485857]
34. Guilbaud M, Piveteau P, Desvaux M, Brisse S, Briandet R. Exploring the diversity of Listeria monocytogenes biofilm architecture by high-throughput confocal laser scanning microscopy and the predominance of the honeycomb-like morphotype. Appl Environ Microbiol. 2015; 81:1813–9. [PubMed: 25548046]
35. Zhao J, Shen Y, Haapasalo M, Wang Z, Wang Q. A 3D numerical study of antimicrobial persistence in heterogeneous multi-species biofilms. J Theor Biol. 2016; 392:83–98. [PubMed: 26739374]
36. Brambilla E, Ionescu A, Cazzaniga G, Ottobelli M. Influence of light-curing parameters on biofilm development and flexural strength of a silorane-based composite. Oper Dent. 2016:219–27. [PubMed: 26266654]
37. Chavez de Paz LE. Image analysis software based on color segmentation for characterization of viability and physiological activity of biofilms. Appl Environ Microbiol. 2009; 75:1734–9. [PubMed: 19139239]
38. Auschill TM, Arweiler NB, Netuschil L, Brecx M, Reich E, Sculean A. Spatial distribution of vital and dead microorganisms in dental biofilms. Arch Oral Biol. 2001; 46:471–6. [PubMed: 11286812]
39. Netuschil L, Reich E, Unteregger G, Sculean A, Brecx M. A pilot study of confocal laser scanning microscopy for the assessment of undisturbed dental plaque vitality and topography. Arch Oral Biol. 1998; 43:277–85. [PubMed: 9839703]
40. Li F, Weir MD, Xu HH. Effects of quaternary ammonium chain length on antibacterial bonding agents. J Dent Res. 2013; 92:932–8. [PubMed: 23958761]

41. Chavez de Paz LE, Resin A, Howard KA, Sutherland DS, Wejse PL. Antimicrobial effect of chitosan nanoparticles on streptococcus mutans biofilms. Appl Environ Microbiol. 2011; 77:3892–5. [PubMed: 21498764]

42. Zhou H, Weir MD, Antonucci JM, Schumacher GE, Zhou XD, Xu HH. Evaluation of three-dimensional biofilms on antibacterial bonding agents containing novel quaternary ammonium methacrylates. Int J Oral Sci. 2014; 6:77–86. [PubMed: 24722581]

43. Simoncic B, Tomsic B. Structures of novel antimicrobial agents for textiles-a review. Textile Research Journal. 2010; 80:1721–37.

44. Murata H, Koepsel RR, Matyjaszewski K, Russell AJ. Permanent, non-leaching antibacterial surface--2: how high density cationic surfaces kill bacterial cells. Biomaterials. 2007; 28:4870–9. [PubMed: 17706762]

45. Engelberg-Kulka H, Amitai S, Kolodkin-Gal I, Hazan R. Bacterial programmed cell death and multicellular behavior in bacteria. PLoS Genet. 2006; 2:e135. [PubMed: 17069462]

46. Gerdes K, Christensen SK, Lobner-Olesen A. Prokaryotic toxin-antitoxin stress response loci. Nat Rev Microbiol. 2005; 3:371–82. [PubMed: 15864262]

47. Beyth N, Yudovin-Farber I, Perez-Davidi M, Domb AJ, Weiss EI. Polyethyleneimine nanoparticles incorporated into resin composite cause cell death and trigger biofilm stress in vivo. Proc Natl Acad Sci U S A. 2010; 107:22038–43. [PubMed: 21131569]

48. Imazato S, Kinomoto Y, Tarumi H, Ebisu S, Tay FR. Antibacterial activity and bonding characteristics of an adhesive resin containing antibacterial monomer MDPB. Dent Mater. 2003; 19:313–9. [PubMed: 12686296]

49. Cheng L, Zhang K, Weir MD, Liu H, Zhou X, Xu HH. Effects of antibacterial primers with quaternary ammonium and nano-silver on Streptococcus mutans impregnated in human dentin blocks. Dent Mater. 2013; 29:462–72. [PubMed: 23422420]

50. Lynch CD, Frazier KB, McConnell RJ, Blum IR, Wilson NH. Minimally invasive management of dental caries: contemporary teaching of posterior resin-based composite placement in U.S. and Canadian dental schools. J Am Dent Assoc. 2011; 142:612–20. [PubMed: 21628682]

51. Frencken JE, Van ‘t Hof MA, Van Amerongen WE, Holmgren CJ. Effectiveness of single-surface ART restorations in the permanent dentition: a meta-analysis. J Dent Res. 2004; 83:120–3. [PubMed: 14742648]

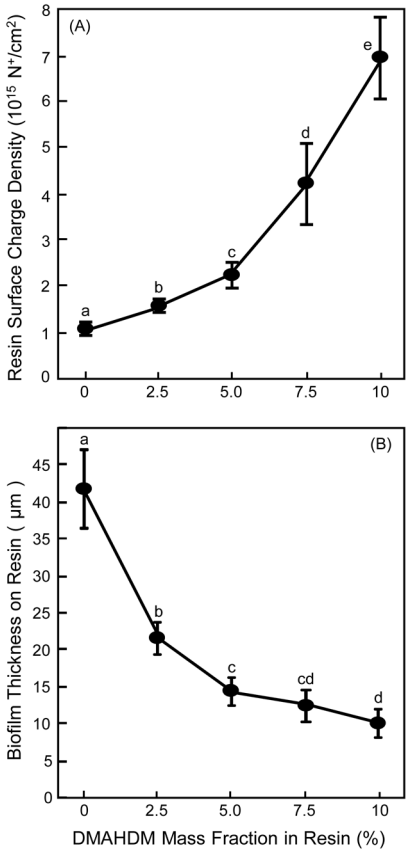

Fig. 1.

Charge density and biofilm thickness on resins: (A) Quaternary amine surface charge density of cured bonding agent resin vs. DMAHDM mass fraction, and (B) biofilm thickness grown for two days on resin (mean ± sd; n = 6). Surface charge density significantly increased with increasing DMAHDM mass fraction. Biofilm thickness decreased with increasing DMAHDM mass fraction. In each plot, values with dissimilar letters are significantly different from each other ($p < 0.05$).

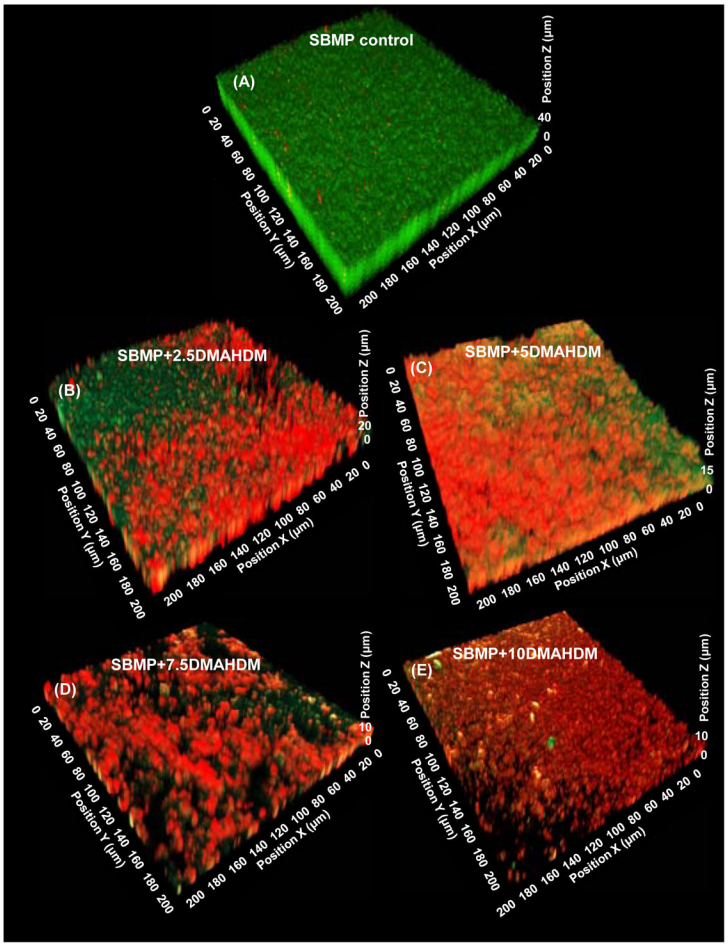

Fig. 2.

Representative CLSM image of 3D biofilms cultured for 2 days on bonding agents: (A) SBMP control, (B) SBMP+2.5DMAHDM, (C) SBMP+5DMAHDM, (D) SBMP +7.5DMAHDM, (E) SBMP+10DMAHDM. The x and x axes are parallel to the resin surface. The z axis is perpendicular to the resin surface. Live bacteria were stained green, and bacteria with compromised membranes were stained red.

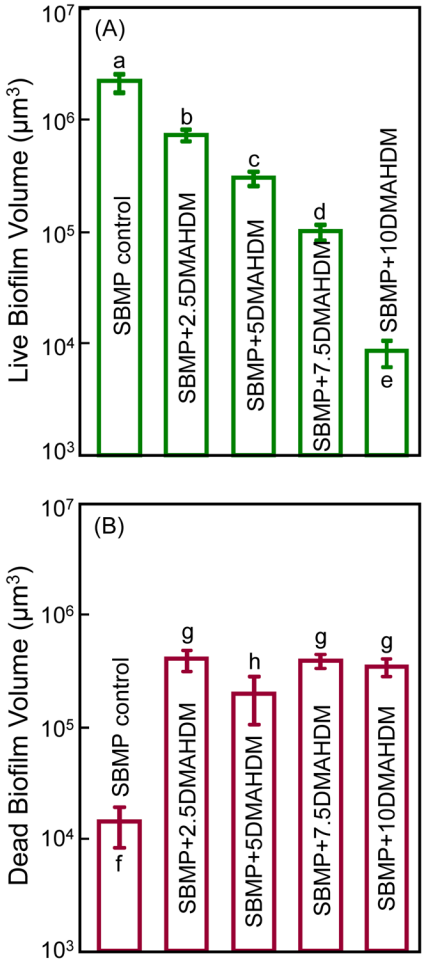

Fig. 3.

Biofilm volume cultured for 2 days on bonding agents: (A) Live biofilm volume, and (B) dead biofilm volume (mean ± sd; n = 6). In each plot, values with dissimilar letters are significantly different from each other ($p < 0.05$).

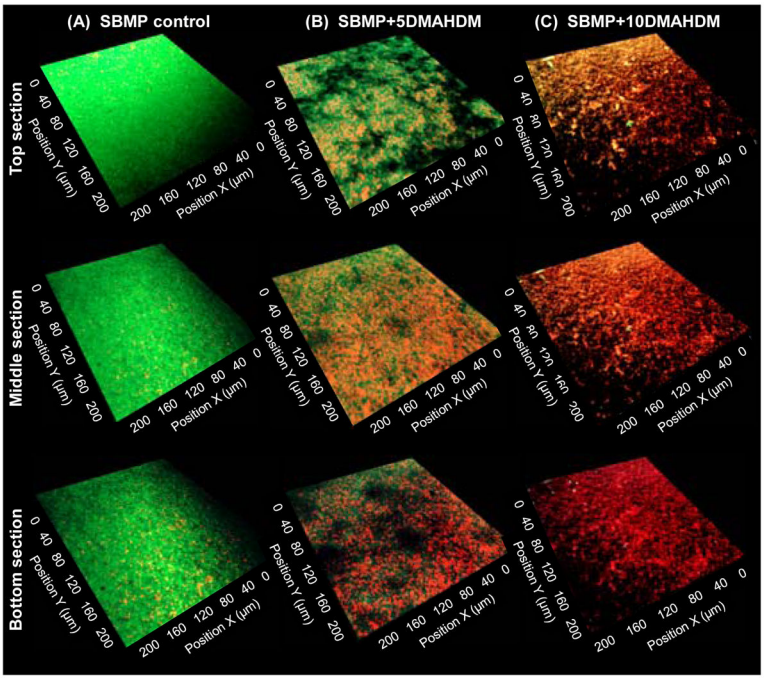

Fig. 4.

Representative 2D live/dead images of cross-sectioned biofilm in the x–y plane. All five bonding agents were tested; shown here are three examples: (A) SBMP control, (B) SBMP +5DMAHDM, (C) SBMP+10DMAHDM. The top labels indicate the materials. The left labels indicate the location of the section in the biofilm: The top biofilm surface, the middle section, and the bottom section (near the resin surface) of the biofilm. Live bacteria were stained green. Bacteria with compromised membranes were stained red.

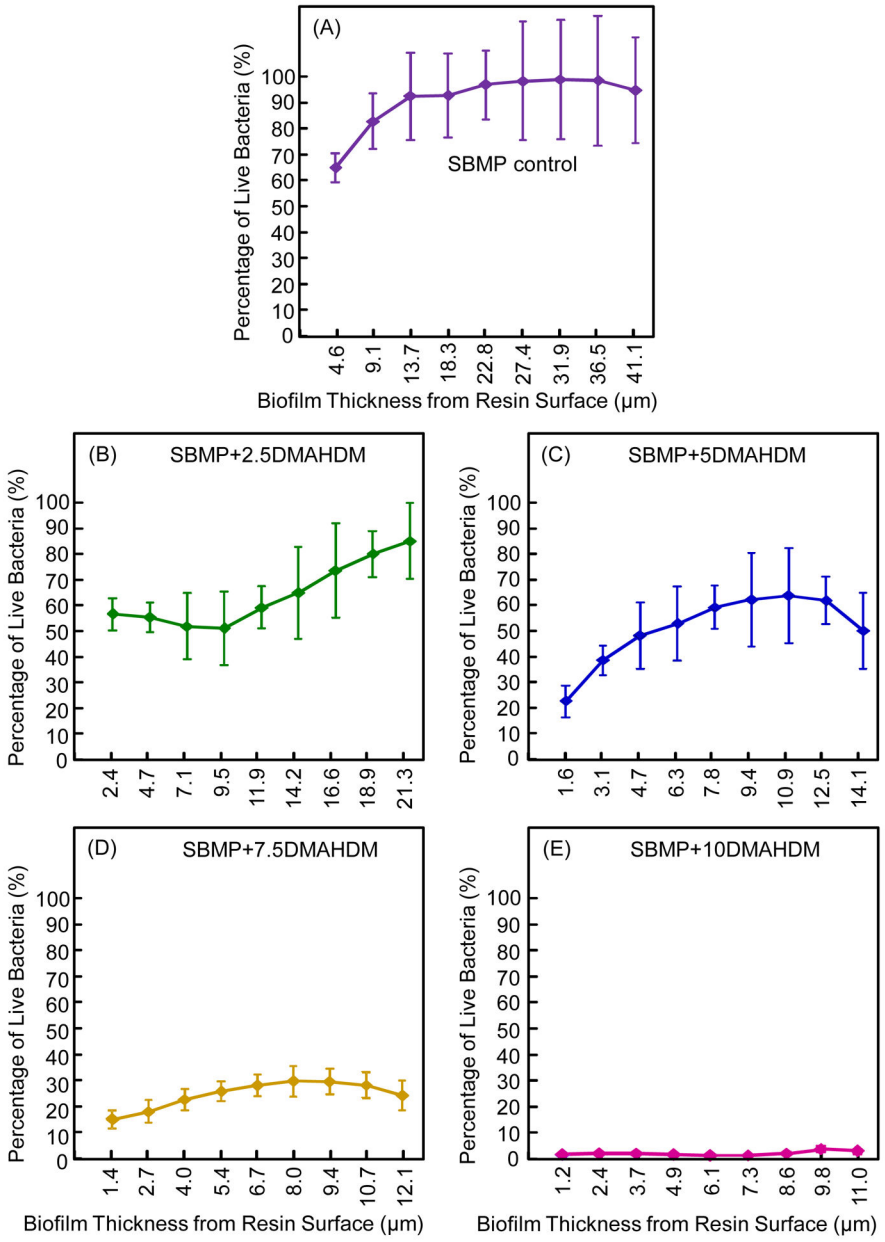

Fig. 5.

Bacterial viability distribution in 3D biofilm (mean ± sd; n = 6): (A) SBMP control, (B) SBMP+2.5DMAHDM, (C) SBMP+5DMAHDM, (D) SBMP+7.5DMAHDM, (E) SBMP +10DMAHDM. Percentage of live bacteria = live bacteria area/(live bacteria area + dead bacteria area). Percentage of live bacteria is plotted vs. the location of the 2D cross-section in the 3D biofilm at a distance measured from the resin surface.

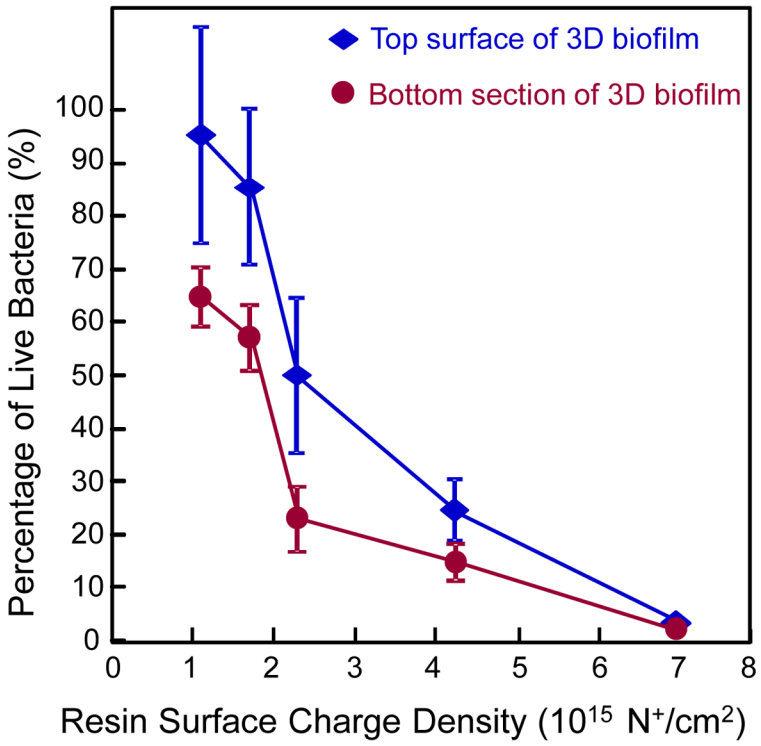

Fig. 6.

Percentage of live bacteria in 3D biofilm vs. resin surface charge density (mean ± sd; n = 6). Two surfaces were measured: Top biofilm surface, and bottom biofilm surface. Percentage of live bacteria decreased with increasing charge density for both surfaces. Percentage of live bacteria is lower at biofilm bottom, and higher in biofilm top surface. Percentage of live bacteria approached 0 for the entire biofilm on SBMP+10DMAHDM.